

Antimicrobial and Antifouling Polymeric Agents for Surface Functionalization of Medical Implants

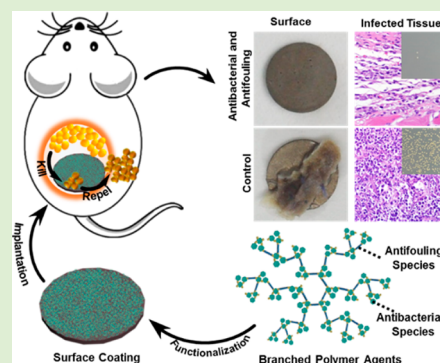
Qiang Zeng,^{†,§} Yiwen Zhu,^{‡,§} Bingran Yu,^{‡,§} Yujie Sun,[†] Xiaokang Ding,^{‡,§} Chen Xu,[‡] Yu-Wei Wu,^{*,†} Zhihui Tang,^{*,†} and Fu-Jian Xu^{*,‡,§}

[†]National Engineering Laboratory for Digital and Material Technology of Stomatology, School and Hospital of Stomatology, Peking University, Beijing 100081, China

[‡]Key Laboratory of Carbon Fiber and Functional Polymers (Beijing University of Chemical Technology), Ministry of Education, Beijing Laboratory of Biomedical Materials, Beijing Advanced Innovation Center for Soft Matter Science and Engineering, Beijing University of Chemical Technology, Beijing 100029, China

Supporting Information

ABSTRACT: Combating implant-associated infections is an urgent demand due to the increasing numbers in surgical operations such as joint replacements and dental implantations. Surface functionalization of implantable medical devices with polymeric antimicrobial and antifouling agents is an efficient strategy to prevent bacterial fouling and associated infections. In this work, antimicrobial and antifouling branched polymeric agents (GPEG and GEG) were synthesized via ring-opening reaction involving gentamicin and ethylene glycol species. Due to their rich primary amine groups, they can be readily coated on the polydopamine-modified implant (such as titanium) surfaces. The resultant surface coatings of Ti-GPEG and Ti-GEG produce excellent *in vitro* antibacterial efficacy toward both *Staphylococcus aureus* and *Escherichia coli*, while Ti-GPEG exhibit better antifouling ability. Moreover, the infection model with *S. aureus* shows that implanted Ti-GPEG possessed excellent antibacterial and antifouling ability *in vivo*. This study would provide a promising strategy for the surface functionalization of implantable medical devices to prevent implant-associated infections.



1. INTRODUCTION

It is of great urgency to combat implant-associated infection,^{1–3} due to the increased use of joint replacements and dental implantations. Among implants, titanium is widely used in orthopedic and dentistry implant prosthesis because of their corrosion resistance, mechanical strength, and great biocompatibility.^{4–7} However, titanium implants are prone to protein adsorption and bacterial fouling after implantation and exposure to body fluids.⁸ The bacterial fouling on the surface of implants may cause serious infection and the biofilm formation makes the bacterial plaques resistant to antibiotics.^{9–11} As a result, strategies are needed to prevent bacterial fouling and biofilm formation on implantable medical devices.^{11–14} Several antibacterial coatings have been reported by using antimicrobial peptides,^{15,16} silver,^{17,18} photodynamic agents,¹⁹ and cationic polymers.^{20,21} However, these surface coatings can easily adsorb proteins, platelets, dead cells, and cell debris under physiological conditions.^{22,23} Therefore, a monofunctional antimicrobial coating is insufficient to prevent biofilm formation.^{24,25} More recently, contact-active antimicrobial and antifouling dual-functional coatings were developed.^{26–28} Such antimicrobial and antifouling agents provide powerful weapons in the arsenal for combating bacterial infections. However, these coatings often require multistep synthetic procedures, which hinders practical application.²⁴ It is

highly desirable to develop one surface coating with potent antimicrobial and antifouling activity via simple procedure.

Herein, we synthesized antibacterial and antifouling branched polymeric agents (GPEG and GEG, Figure 1) via a one-pot ring-opening reaction of traditional antibiotic gentamicin with poly(ethylene glycol) (PEG) species containing diepoxy groups. As a broad-spectrum commercial antimicrobial agent, gentamicin exhibits efficient antibacterial activities against both *Escherichia coli* and *Staphylococcus aureus*.^{24,29} Meanwhile, the PEG moieties render the antifouling capability.^{11,30–32} Due to their rich primary amine groups, the proposed GPEG and GEG agents also can be easily coated onto medical implants (such as titanium disk) pretreated with a mussel-inspired polydopamine (PDA) adhesive layer.^{33,34} It can be expected that such polymeric coatings on the Ti disks will exhibit potent antibacterial activity and significantly inhibit the growth of biofilms. The *in vitro* biological properties of surface coatings, including antimicrobial activities and inhibition of biofilm were investigated in detail. An animal model with the implant-associated infection was also established, and the antibacterial

Received: March 6, 2018

Revised: May 2, 2018

Published: May 4, 2018

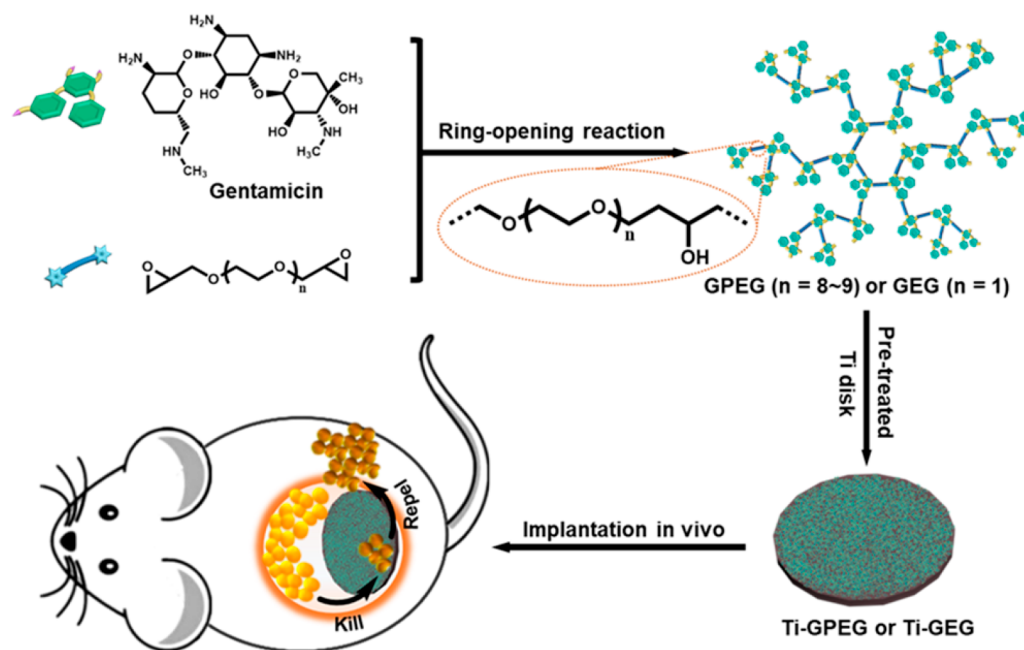


Figure 1. Schematic illustration of the synthetic route of antibacterial and antifouling polymeric agents and their application for the surface functionalization of medical implants.

and antifouling ability of the polymer-modified Ti disks was studied *in vivo*.

2. EXPERIMENTAL SECTION

2.1. Materials. Gentamicin sulfate (98%), poly(ethylene glycol) diglycidyl ether (PEGDGE), ethylene glycoldiglycidyl ether (EGDE, 98%), ethylenediamine (ED, 98%) and sodium periodate were purchased from Sigma-Aldrich. Dopamine hydrochloride was obtained from Energy Chemical (Shanghai, China). Dimethyl sulfoxide (DMSO, A.R. grade) was purchased from Beijing Chemical Works (China). The pathological glass slides were purchased from Citotest (Jiangsu, China). Tryptone and yeast extract were brought from Oxoid (UK). The strains of *Escherichia coli* (*E. coli*, JM 109) and *Staphylococcus aureus* (FRF 1169) were obtained from Promega (Madison, USA). The Live/Dead BacLight bacterial viability kit (L7012) was purchased from Invitrogen (LifeTechnologies, USA). The lysogeny broth (LB) medium and deionized water were autoclaved (120 °C, 20 min) before use. The Cell Counting Kit-8 (CCK-8) was purchased from Wobisen Technology Co (Beijing, China). The Ti disks with a diameter of 10 mm and the thickness of 0.5 mm were obtained from Hailihua Biotechnology Limited Company (Guangzhou, China).

2.2. Synthesis of Polymeric Agents. First, commercial gentamicin was desulfated as described in our earlier work.²⁷ The antibacterial and antifouling polymers were synthesized via ring-opening reaction, namely GPEG (from gentamicin and PEGDGE) and GEG (from gentamicin and EGDE). The antifouling analogue (EPEG) was prepared by ring-opening reaction between ED and epoxy groups of PEGDGE. The detailed synthetic procedures and characterization are described in the [Supporting Information](#).

2.3. Polymeric Coatings on Ti Disks and Characterization. For the preparation of antibacterial and antifouling coatings, the Ti disks were pretreated in a Tris(hydroxymethyl)aminomethane hydrochloride (Tris-HCl) buffer solution (10 mM, pH 8.5) containing 2 mg/mL of dopamine. After overnight incubation, a layer of polydopamine (PDA) was coated on the surface of Ti disks, and the resultant Ti disks were rinsed with copious deionized water to remove unreacted reagents. Then, the pretreated Ti disks were transferred into 1 mL of aqueous solution containing 1 mg/mL of sodium periodate to activate the PDA film. After 10 min, the activated Ti disks were washed with deionized water and immediately transferred into the aqueous

solutions containing EPEG, GEG and GPEG (2 mg/mL), respectively. After the incubation at 55 °C for 5 h, all the Ti disks with different coatings (namely Ti-EPEG, Ti-GEG, and Ti-GPEG) were rinsed with a copious amount of deionized water and dried with nitrogen gas. The pretreated Ti disks without activation were used as the control group.

X-ray photoelectron spectroscopy (XPS) spectra were recorded on a Kratos AXIS HSi spectrometer (Kratos Analytical Ltd., UK) equipped with a monochromatized Al K α X-ray source (1486.6 eV photons) to characterize modified-Ti disks. The static water contact angles (WCAs) of samples were measured with Dataphysics OCA system (Dataphysics, Germany) at room temperature. Two microliters of deionized water was dispensed onto Ti disks or modified Ti disks, and the WCAs on the samples were measured and recorded at least three times.

2.4. Antibacterial Assay. The antibacterial activity of each polymer in solution was evaluated with inhibition efficiency and minimum inhibitory concentration (MIC), which was described in detail in [Supporting Information](#). To examine the antibacterial and antifouling abilities of polymer-coated surfaces, the Ti disks with different antibacterial coatings were incubated in bacteria culture, and subjected to live/dead staining. The detailed procedures are described in the [Supporting Information](#).

2.5. Inhibition of Biofilm Formation. All the modified Ti disks were incubated in LB medium (5 mL) containing 1×10^8 cfu/mL of bacteria (*S. aureus* or *E. coli*) at a stationary atmosphere at 37 °C to allow biofilm formation. After 7 days, all disks were washed with phosphate buffer saline (PBS) solution under aseptic condition to remove the medium and unbound bacteria. Then, the disks were incubated in a staining solution containing SYTO 9 (6 μ mol/L) and propidium iodide (PI, 30 μ mol/L) from live/dead staining kit (L7012) in the dark. After 15 min, the stained bacteria were imaged by 3D confocal laser scanning microscope (CLSM, Leica, SP8) using an oil immersed 63 \times objective lens.

2.6. In Vivo Anti-Infection Assay. Female BALB/c mice aged 8 weeks with body weight around 20 g were used for *in vivo* anti-infection assay. All protocols involving the mice comply with the guidelines described in the Association for Assessment and Accreditation of Laboratory Animal Care, approved by the Peking University Health Centre Institutional Animal Care and Use Committee and Peking University Health Centre Ethics Committee. The surgical operations were performed after one-week adaption. All

the mice were divided into five groups: (1) with infection and Ti-GPEG; (2) with infection and Ti-GEG; (3) with infection and Ti-EPEG; (4) with infection and pretreated Ti (control (+)); and (5) just with pretreated Ti (control (-)). The mice were anesthetized by intraperitoneal injection of 1% pentobarbital sodium (75:1 mg/kg). Then, a 0.8–1.0 cm incision was cut parallel to the spine, and the autoclave sterilized Ti disks were implanted subcutaneously. After the incision was closed with 4–0 sutures, 100 μ L of *S. aureus* suspension (1×10^7 cfu/mL) was subcutaneously administrated to the implantation site under the Ti disk. The skin temperatures of mice were monitored on a daily basis throughout the experiment. On the 1st, 4th, 7th, and 14th day after surgery, six mice of each group were sacrificed by overdose pentobarbital sodium administration. Ti disks and the soft tissues around Ti disks of the sacrificed mice were harvested. The *ex vivo* Ti disks were incubated in PBS buffer solution, and stained with live/dead BacLight Bacterial Viability Kit, and the bacteria were imaged by CLSM. Soft tissues around the disk were obtained, weighed, and homogenized in normal saline (1 mg/mL) using a high-speed homogenizer (IKA T25, Germany). The homogenates were sequentially diluted with normal saline. The diluted tissue homogenates were spread on LB-agar plates and incubated at 37 °C. After 24 h, the bacterial plaques on the plate were counted. The DNA of single-colony bacteria on the plate was amplified by polymerase chain reaction (PCR) with bacterial universal primer 27F (AGAGTTTGATCCTGGCTCAG) and 1492R (TACGGCTACCTTGTTACGACTT). Full length of 16S rDNA was sequenced and compared with sequences in National Center for Biotechnology Information (NCBI) database by Basic Local Alignment Search Tool (BLAST). Soft tissues around the disk were collected and fixed in 4% paraformaldehyde, dehydrated, and embedded in paraffin. The tissues were cut into 5 μ m slices and stained with hematoxylin-eosin (H&E) according to the standard protocols.

2.7. Statistical Analysis. The experimental data were presented as means \pm standard deviation with at least triplicate measurements. A detailed statistical analysis is described in the Supporting Information.

3. RESULTS AND DISCUSSION

3.1. Preparation and Characterization of Polymeric Agents. The antibacterial and antifouling agents were synthesized via ring-opening reaction of the amine groups of gentamicin with the diepoxide group (of ethylene glycol diglycidyl ether (EGDE) or poly(ethylene glycol) diglycidyl ether (PEGDGE)), namely GEG (from gentamicin and EGDE) and GPEG (from gentamicin and PEGDGE) (Figure 1). The antifouling analogue (EPEG, Figure S1 in Supporting Information) was synthesized via the ring-opening reaction of ethylenediamine (ED) with PEGDGE). ^1H NMR was used to characterize the structures of polymers (Figure S2, Supporting Information). For GPEG and GEG, the chemical shift (δ) at $\delta = 3.61$ was attributed to the PEG moieties, and the peaks (a,c,d) from 2.50 to 4.25 were attributed to the methyl groups of gentamicin and the methylene protons (N-CH₂-CH) and (O-CH₂-CH). For EGPG, the peak (e) at $\delta = 3.61$ also shows the featured chemical shifts of protons of PEG moieties. The peaks at 2.51–3.03 and 3.72–4.05 were attributed to the methylene protons (N-CH₂-CH) and (O-CH₂-CH). The methylene protons (O-CH₂-CH₂) belong to PEG moieties predominate the signal ratio, causing other signals to be relatively low. More signal peaks were probably because the gentamicin possesses different chemical environments in the polymer. The number-average molecular weight (M_n) of GPEG, GEG, and EPEG were 5.8×10^3 g mol⁻¹, 3.4×10^3 g mol⁻¹, and 3.8×10^3 g mol⁻¹ with the corresponding polydispersity indexes (PDI) of 1.37, 1.24 and 1.54, respectively. The elemental analysis was done to certify the

percentage of gentamicin incorporated into polymers. The mass percentages of gentamicin of GPEG and GEG are 15.2% and 53.6%, respectively (Table S1, Supporting Information).

3.2. Antibacterial Activity in Solution. The antimicrobial activity of the polymers toward both the Gram-positive bacteria (*S. aureus*) and Gram-negative bacteria (*E. coli*) were studied in solution (Figure 2). For *S. aureus*, the minimum inhibitory

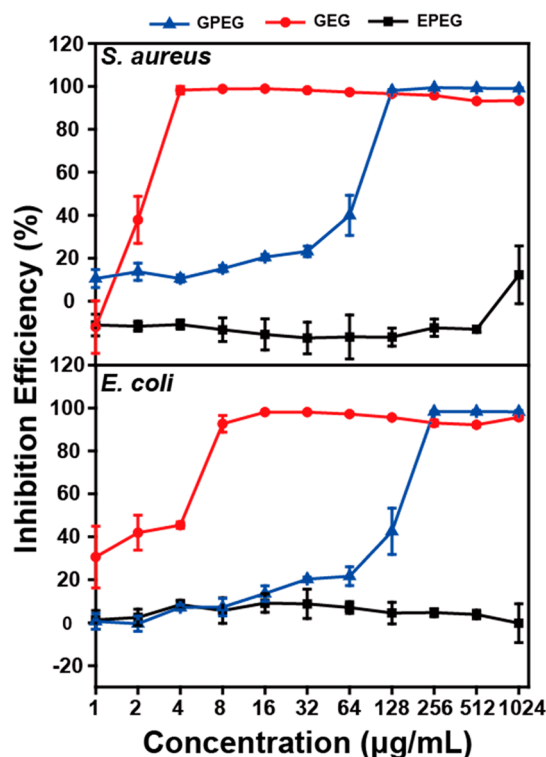


Figure 2. Inhibition efficiencies of the antibacterial polymers against *S. aureus* and *E. coli*, respectively. The error bars indicate the standard deviation ($n = 3$).

concentration (MIC) values of GEG and GPEG are $4 \mu\text{g mL}^{-1}$ and $128 \mu\text{g mL}^{-1}$, respectively. For *E. coli*, the MIC values of GEG and GPEG are $8 \mu\text{g mL}^{-1}$ and $256 \mu\text{g mL}^{-1}$, respectively. GEG shows much lower MIC than GPEG, because GEG has a larger proportion of gentamicin than that of GPEG (Table S1, Supporting Information). Figure 2 also shows that EPEG exhibits minimal antibacterial activity.

3.3. Physical Characterizations of Surface Coatings.

The pretreated Ti disks with PDA were used as the control in this work. All disks (modified with GPEG, GEG, and EPEG, namely Ti-GPEG, Ti-GEG, Ti-EPEG surfaces, respectively) were characterized by XPS spectra (Figure S3, Supporting Information). Ti-GPEG has the highest ratio of C–O peak (66.2%), followed by Ti-GEG with a C–O peak (51.6%), attributed to the PEG moieties in the polymer structure. Meanwhile, Ti-EPEG has the highest percentage of C–N peak (18.7%), owing to the higher percentage of the C–N bond of ED. The above results confirmed the successful coatings of three different polymers on Ti disks. The hydrophilicity of the modified Ti disks was further examined by WCA. Figure S4 (Supporting Information) shows the changes in the contact angles of disks before and after modification. Pristine Ti disks were hydrophobic with a contact angle of 91.6° . After pretreatment with PDA, the contact angle decreased to 51.5° , indicating that the surface became more hydrophilic. All the

surfaces of Ti-GPEG, Ti-GEG, and Ti-EPEG show contact angles around 45°, also showing the successful modification of the Ti disks.

3.4. Antibacterial and Antifouling Abilities of Polymer-Coated Disks. To examine the antibacterial and antifouling abilities of polymer-coated surfaces, the Ti disks with different coatings were characterized by the live/dead staining and scanning electron microscope (SEM). **Figure 3**

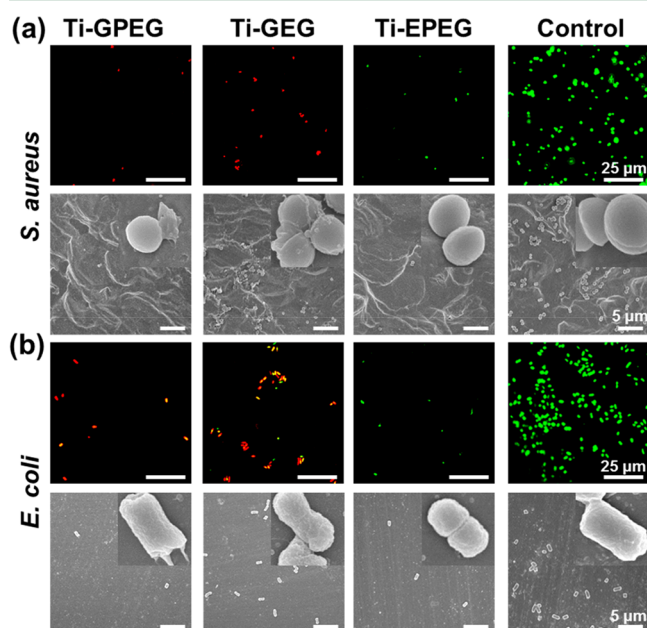


Figure 3. CLSM and SEM images of *S. aureus* (a) and *E. coli* (b) on the modified Ti disks.

shows the fluorescent and SEM images of *S. aureus* and *E. coli* on each disk. On the pretreated Ti disks (control), only green fluorescence stained *S. aureus* and *E. coli* can be observed, showing that the pretreated Ti disks exhibit minimal antibacterial activity. When *E. coli* and *S. aureus* were treated with Ti-GEG and Ti-GPEG, almost all of the bacteria were killed. By contrast, all bacteria were still alive when the bacteria cultures were incubated with Ti-EPEG. The antibacterial ability is caused by the gentamicin species. In addition, fewer *S. aureus* and *E. coli* remained on the surface of Ti-EPEG, Ti-GEG, and Ti-GPEG than the control disk, indicating the good antifouling abilities of Ti-EPEG, Ti-GEG, and Ti-GPEG due to the PEG moieties. Moreover, Ti-EPEG and Ti-GPEG retain less *E. coli* and *S. aureus* colonies compared with Ti-GEG. The SEM images in **Figure 3** show the morphologies of *S. aureus* and *E. coli*. On the Ti-EPEG and control surfaces, *S. aureus* and *E. coli* cells show regular and smooth shapes, while the membrane collapse and shape deformation were observed in the bacteria cells on the Ti-GPEG or Ti-GEG surfaces.

3.5. Inhibition of Biofilm Formation. Inhibition of biofilms is one of the most important properties to prevent implant-associated infections. The three-dimensional (3D) confocal laser scanning microscopy (CLSM) images of bacterial colonies on disks after 7 day incubation are shown in **Figure 4**. A large number of live cells were observed on the control surface with the thickness of 4 μm for *S. aureus* and 8 μm for *E. coli*, respectively. The surface coated with GPEG and EPEG had significantly less bacterial fouling as compared with Ti-GEG, which is in agreement with the viable surface colonies in **Figure**

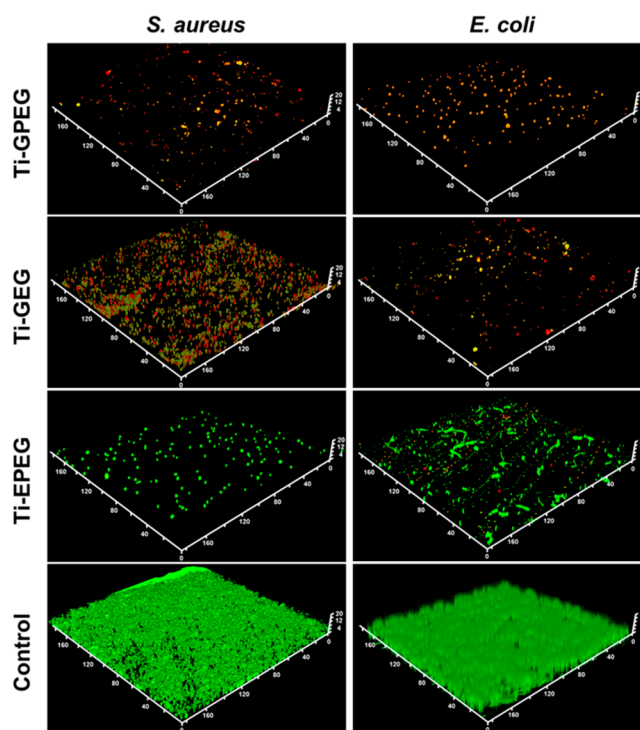


Figure 4. 3D CLSM images of the biofilms on the modified Ti disks for 7 days.

3. In addition, Ti-GPEG and Ti-GEG displayed more dead cells compared with Ti-EPEG. The above results indicated that Ti-GPEG demonstrated great promise in inhibiting biofilm formation. The antibacterial polymer was grafted onto the dopamine modified Ti disks via a Schiff base reaction. Zone of Inhibition (ZOI) determination is a method for detecting the dissolution/nondissolution of antibacterial materials.³⁵ No zone of inhibition was observed (**Figure S5** in the **Supporting Information**), indicating that the grafted polymer was stable on the Ti disks.

3.6. In Vivo Anti-Infection Assay. To evaluate the antibacterial and antifouling properties *in vivo*, an animal model for the implant-associated infection was established. The mice were observed for 14 days to obtain an acute to the chronic infection progression. The skin temperatures of mice fluctuated within normal range (**Figure S4**, **Supporting Information**). After 14 days of suture closure, the wound sites of the Ti-GEG and Ti-GPEG groups healed well, and no obvious redness or swelling was observed (**Figure 5**). By contrast, the Ti-EPEG and control (+) groups showed a delayed wound healing and appeared swollen. Meanwhile, the *ex vivo* Ti disks of the Ti-EPEG and control (+) groups were covered with pus. The fluorescence images show more bacteria fouling on the control (+) surface, while less on the Ti-GPEG surface. Some unidentified cells and debris can be seen in the control (−) group.³⁶ The used Live/Dead bacterial staining kit (Invitrogen, L7012) contains SYTO 9 and PI (propidium iodide). The kit also can stain prokaryotic and eukaryotic cells.^{37,38} Ti-EPEG, Ti-GEG and Ti-GPEG possess good antifouling abilities, which accounts for less amount of cells and debris. The above results suggest the superior antifouling property of the Ti-GPEG group.

The number of bacteria around modified Ti disks was determined by counting the bacterial colonies on the LB-agar

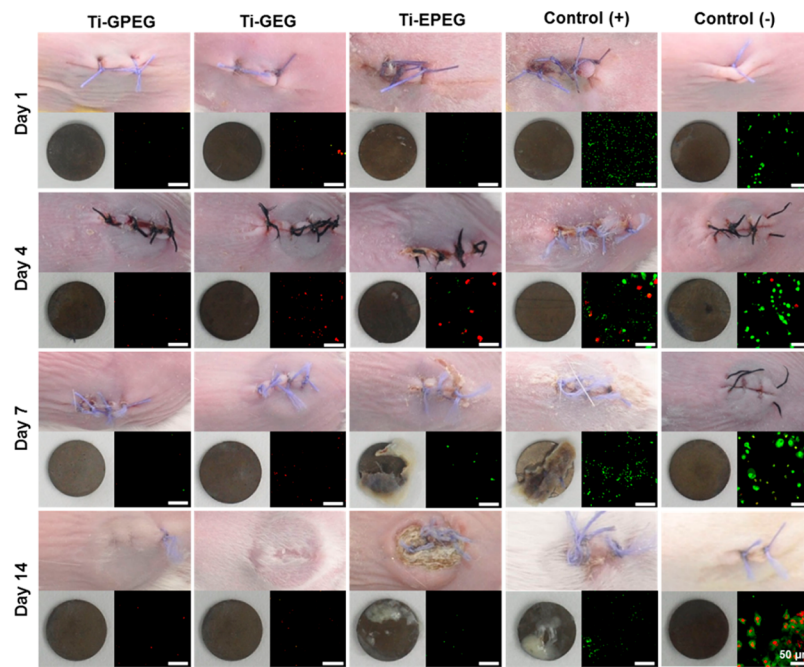


Figure 5. Wound photographs of different groups of mice after implant experiment, ex vivo Ti disk photos and fluorescence imaging of live/dead bacteria staining after 1–14 days.

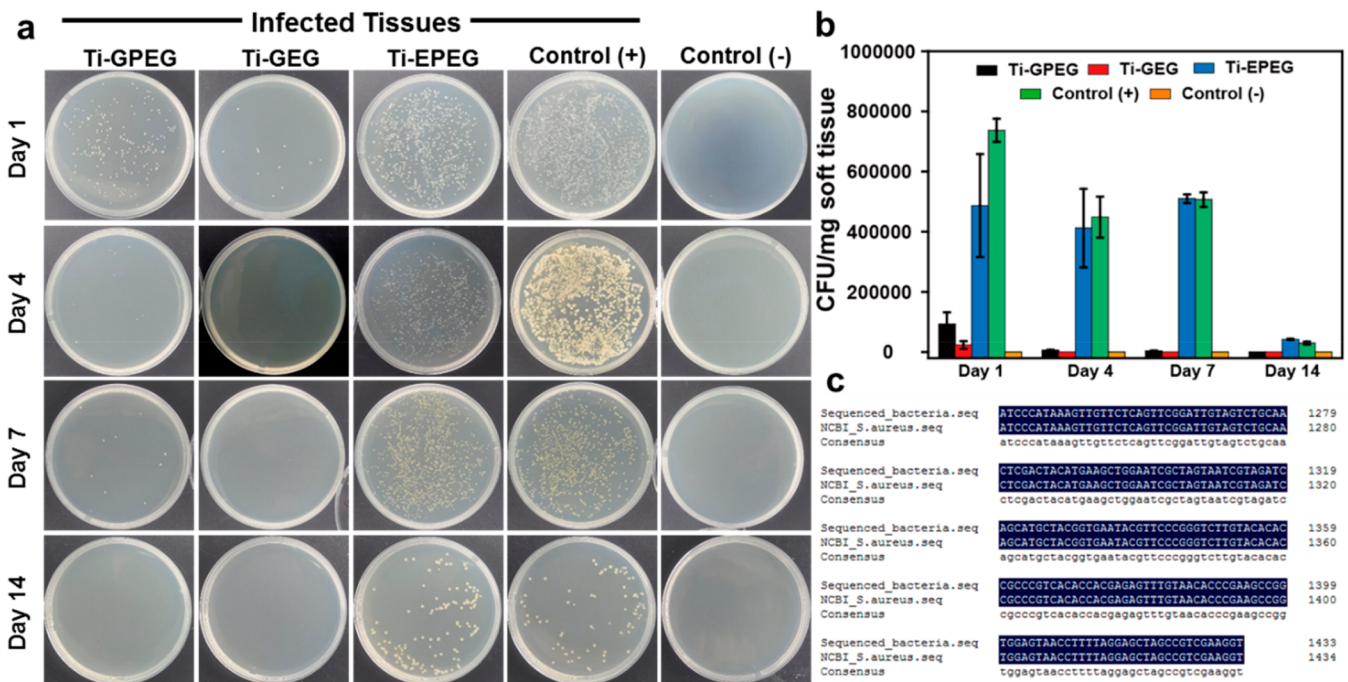


Figure 6. Plate counting photos (a) and number of viable bacteria (b) in soft tissues around the Ti disks in the subcutaneous infection model after 1–14 days. (c) Parts of the 16S rDNA sequencing results of the bacteria (from the infected soft tissues) compared with sequences in NCBI database.

plate (Figure 6a and 6b). After the implantation for 1 day, the bacteria numbers on Ti-GPEG and Ti-GEG were significant less than the Ti-EPEG and control (+) groups. After 4, 7, and 14 days, the number of bacteria grown on the LB-agar plate gradually decreased in the Ti-GPEG and Ti-GEG groups. The number of bacteria in the control (+) group showed a slow decrease after 7 and 14 days. Such phenomenon is probably caused by the spontaneous immune response and suppuration. Bacteria number in the Ti-EPEG group remained slightly higher in the progression, because Ti-EPEG does not have

antibacterial ability. The DNA sequence of the bacteria grown on the LB-agar plate corresponded 99% with *S. aureus* in NCBI database (Figure 6c and Figure S7 in the Supporting Information). In addition, no bacterial colonies were observed in the control (–) group, further indicating that the stained species in Figure 5 were from unidentified cells and debris.

The infected tissues of the mice were harvested and subjected to hematoxylin and eosin (H&E) staining. Prominent neutrophilic infiltration responses in the Ti-EPEG and control (+) groups were observed after 1 day, indicating an acute

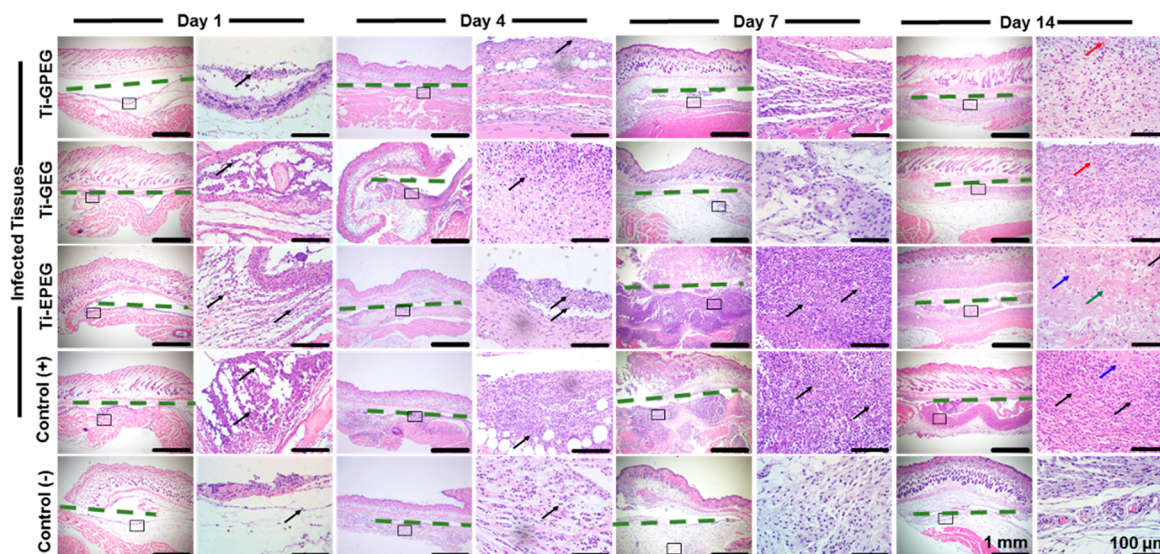


Figure 7. Representative images of tissue section around the Ti disks stained with H&E after 1–14 days. Green dashes represent Ti disk location (Arrows: black, neutrophils; red, newly formed vessels and granuloma; green: necrosis; blue: fibrinous inflammation).

inflammatory response (Figure 7). The amount of neutrophil in the Ti-GPEG and Ti-GEG groups is smaller, showing a milder inflammatory response. Some neutrophil could also be found in the control (–) group due to the Ti disk implantation procedure.³⁹ 7 days later, the neutrophil infiltration decreased in the control (–), Ti-GPEG and Ti-GEG groups, while in the other two groups the infiltration became more severe and disintegrated neutrophil could be observed. After 14 days, the necrosis took place in the Ti-EPEG and control (+) groups, which is in accordance with the actual situation of the mice after implantation. No obvious neutrophil remained in the tissue of the Ti-GPEG group. Meanwhile, the granulomatous inflammation and newly formed vessels occurred and fibroblasts presented as well, showing a healing process.

4. CONCLUSIONS

In summary, antibacterial and antifouling polymeric agents (GPEG and GEG) have been successfully synthesized via ring-opening reaction. GPEG and GEG show excellent antibacterial activity due to the gentamicin moieties in the polymer structures. Owing to their rich primary amine groups, antibacterial and antifouling polymers can also be coated on Ti disks via an adhesive PDA layer. The *in vitro* and *in vivo* anti-infection assays prove that Ti-GPEG possesses significant antibacterial and antifouling ability. This work would provide a promising approach for the effective surface functionalization of medical implants to reduce implant-associated infections.

■ ASSOCIATED CONTENT

Supporting Information

The Supporting Information is available free of charge on the ACS Publications website at DOI: 10.1021/acs.biomac.8b00399.

Detailed experimental method, synthesis routes of EPEG, ¹H NMR spectra, XPS spectra, water contact angles, mice skin temperature, and gene sequence of bacteria (PDF)

■ AUTHOR INFORMATION

Corresponding Authors

*Tel.: 8610-64421243; E-mail address: yuweiwu@bjmu.edu.cn (Y.-W.W.).

*E-mail: zihui_tang@126.com (Z.T.).

*E-mail: xufj@mail.buct.edu.cn (F.J.X.).

ORCID

Bingran Yu: 0000-0003-4912-5632

Xiaokang Ding: 0000-0002-6705-4148

Fu-Jian Xu: 0000-0002-1838-8811

Author Contributions

§These authors contributed equally to this work.

Notes

The authors declare no competing financial interest.

■ ACKNOWLEDGMENTS

This work was partially supported by National Key Research and Development Program of China (Grant Numbers 2016YFB1101200 and 2016YFC1100404), National Natural Science Foundation of China (Grant Numbers 81300851, 51733001, and 51503012), and Beijing Natural Science Foundation (Project No. 7161001).

■ REFERENCES

- (1) Hickok, N. J.; Shapiro, I. M.; Chen, A. F. The Impact of Incorporating Antimicrobials into Implant Surfaces. *J. Dent. Res.* **2018**, *97*, 14–22.
- (2) Bauer, S.; Schmuki, P.; von der Mark, K.; Park, J. Engineering Biocompatible Implant Surfaces Part I: Materials and Surfaces. *Prog. Mater. Sci.* **2013**, *58*, 261–326.
- (3) Dong, A.; Wang, Y.-J.; Gao, Y.; Gao, T.; Gao, G. Chemical Insights into Antibacterial *N*-Halamines. *Chem. Rev.* **2017**, *117*, 4806–4862.
- (4) Liao, H.; Miao, X.; Ye, J.; Wu, T.; Deng, Z.; Li, C.; Jia, J.; Cheng, X.; Wang, X. Falling Leaves Inspired ZnO Nanorods–Nanoslices Hierarchical Structure for Implant Surface Modification with Two Stage Releasing Features. *ACS Appl. Mater. Interfaces* **2017**, *9*, 13009–13015.
- (5) Hu, Y.; Cai, K.; Luo, Z.; Jandt, K. D. Layer-by-Layer Assembly of β -estradiol Loaded Mesoporous Silica Nanoparticles on Titanium

Substrates and Its Implication for Bone Homeostasis. *Adv. Mater.* **2010**, *22*, 4146–4150.

(6) Zhou, R.; Wei, D.; Cao, J.; Feng, W.; Cheng, S.; Du, Q.; Li, B.; Wang, Y.; Jia, D.; Zhou, Y. Synergistic Effects of Surface Chemistry and Topologic Structure from Modified Microarc Oxidation Coatings on Ti Implants for Improving Osseointegration. *ACS Appl. Mater. Interfaces* **2015**, *7*, 8932–8941.

(7) Nayak, S.; Dey, T.; Naskar, D.; Kundu, S. C. The Promotion of Osseointegration of Titanium Surfaces by Coating with Silk Protein Sericin. *Biomaterials* **2013**, *34*, 2855–2864.

(8) Liu, Z.; Ma, S.; Duan, S.; Xuliang, D.; Sun, Y.; Zhang, X.; Xu, X.; Guan, B.; Wang, C.; Hu, M.; Qi, X.; Zhang, X.; Gao, P. Modification of Titanium Substrates with Chimeric Peptides Comprising Antimicrobial and Titanium-Binding Motifs Connected by Linkers to Inhibit Biofilm Formation. *ACS Appl. Mater. Interfaces* **2016**, *8*, 5124–5136.

(9) Xu, L.; Pranantyo, D.; Neoh, K.-G.; Kang, E.-T.; Teo, S. L.-M.; Fu, G. D. Synthesis of Catechol and Zwitterion-Bifunctionalized Poly(Ethylene Glycol) for The Construction of Antifouling Surfaces. *Polym. Chem.* **2016**, *7*, 493–501.

(10) Liu, Y.; van der Mei, H. C.; Zhao, B.; Zhai, Y.; Cheng, T.; Li, Y.; Zhang, Z.; Busscher, H. J.; Ren, Y.; Shi, L. Eradication of Multidrug-Resistant Staphylococcal Infections by Light-Activatable Micellar Nanocarriers in A Murine Model. *Adv. Funct. Mater.* **2017**, *27*, 1701974.

(11) Zander, Z. K.; Becker, M. L. Antimicrobial and Antifouling Strategies for Polymeric Medical Devices. *ACS Macro Lett.* **2018**, *7*, 16–25.

(12) Shi, Z.-Q.; Cai, Y.-T.; Deng, J.; Zhao, W.-F.; Zhao, C.-S. Host-Guest Self-Assembly Toward Reversible Thermoresponsive Switching for Bacteria Killing and Detachment. *ACS Appl. Mater. Interfaces* **2016**, *8*, 23523–23532.

(13) Muñoz-Bonilla, A.; Fernández-García, M. Polymeric Materials with Antimicrobial Activity. *Prog. Polym. Sci.* **2012**, *37*, 281–339.

(14) Muñoz-Bonilla, A.; Fernández-García, M. The Roadmap of Antimicrobial Polymeric Materials in Macromolecular Nanotechnology. *Eur. Polym. J.* **2015**, *65*, 46–62.

(15) He, J.; Chen, J.; Hu, G.; Wang, L.; Zheng, J.; Zhan, J.; Zhu, Y.; Zhong, C.; Shi, X.; Liu, S.; Wang, Y.; Ren, L. Immobilization of an Antimicrobial Peptide on Silicon Surface with Stable Activity by Click Chemistry. *J. Mater. Chem. B* **2018**, *6*, 68–74.

(16) Wang, L.; Chen, J.; Shi, L.; Shi, Z.; Ren, L.; Wang, Y. The Promotion of Antimicrobial Activity on Silicon Substrates using a “Click” Immobilized Short Peptide. *Chem. Commun.* **2014**, *50*, 975–977.

(17) Khachatryan, G.; Khachatryan, K.; Grzyb, J.; Fiedorowicz, M. Formation and Properties of Hyaluronan/Nano Ag and Hyaluronan-Lecithin/Nano Ag Films. *Carbohydr. Polym.* **2016**, *151*, 452–457.

(18) Gao, C.; Wang, Y.; Han, F.; Yuan, Z.; Li, Q.; Shi, C.; Cao, W.; Zhou, P.; Xing, X.; Li, B. Antibacterial Activity and Osseointegration of Silver-Coated Poly(Ether Ether Ketone) Prepared Using the Polydopamine-Assisted Deposition Technique. *J. Mater. Chem. B* **2017**, *5*, 9326–9336.

(19) Zhu, Y.; Xu, C.; Zhang, N.; Ding, X.; Yu, B.; Xu, F.-J. Polycationic Synergistic Antibacterial Agents with Multiple Functional Components for Efficient Anti-Infective Therapy. *Adv. Funct. Mater.* **2018**, *28*, 1706709.

(20) Guo, J.; Xu, Q.; Zheng, Z.; Zhou, S.; Mao, H.; Wang, B.; Yan, F. Intrinsically Antibacterial Poly(Ionic Liquid) Membranes: the Synergistic Effect of Anions. *ACS Macro Lett.* **2015**, *4*, 1094–1098.

(21) Liu, S.; Ono, R. J.; Wu, H.; Teo, J. Y.; Liang, Z. C.; Xu, K.; Zhang, M.; Zhong, G.; Tan, J. P.K.; Ng, M.; Yang, C.; Chan, J.; Ji, Z.; Bao, C.; Kumar, K.; Gao, S.; Lee, A.; Fevre, M.; Dong, H.; Ying, J. Y.; Li, L.; Fan, W.; Hedrick, J. L.; Yang, Y. Y. Highly Potent Antimicrobial Polyionenes with Rapid Killing Kinetics, Skin Biocompatibility and in Vivo Bactericidal Activity. *Biomaterials* **2017**, *127*, 36–48.

(22) Banerjee, I.; Pangule, R. C.; Kane, R. S. Antifouling Coatings: Recent Developments in the Design of Surfaces that Prevent Fouling by Proteins, Bacteria, and Marine Organisms. *Adv. Mater.* **2011**, *23*, 690–718.

(23) Yu, Q.; Zhang, Y.; Wang, H.; Brash, J.; Chen, H. Anti-Fouling Bioactive Surfaces. *Acta Biomater.* **2011**, *7*, 1550–1557.

(24) Zhi, Z.; Su, Y.; Xi, Y.; Tian, L.; Xu, M.; Wang, Q.; Padidan, S.; Li, P.; Huang, W. Dual-Functional Polyethylene Glycol Polyhexanide Surface Coating with in Vitro and in Vivo Antimicrobial and Antifouling Activities. *ACS Appl. Mater. Interfaces* **2017**, *9*, 10383–10397.

(25) Liu, R.; Chen, X.; Falk, S. P.; Masters, K. S.; Weisblum, B.; Gellman, S. H. Nylon-3 Polymers Active Against Drug-Resistant *Candida Albicans* Biofilms. *J. Am. Chem. Soc.* **2015**, *137*, 2183–2186.

(26) Ding, X.; Yang, C.; Lim, T. P.; Hsu, L. Y.; Engler, A. C.; Hedrick, J. L.; Yang, Y.-Y. Antibacterial and Antifouling Catheter Coatings Using Surface Grafted PEG-*b*-Cationic Polycarbonate Diblock Copolymers. *Biomaterials* **2012**, *33*, 6593–6603.

(27) Voo, Z. X.; Khan, M.; Xu, Q.; Narayanan, K.; Ng, B. W. J.; Bte Ahmad, R.; Hedrick, J. L.; Yang, Y. Y. Antimicrobial Coatings Against Biofilm Formation: the Unexpected Balance between Antifouling and Bactericidal Behavior. *Polym. Chem.* **2016**, *7*, 656–668.

(28) Gao, Q.; Li, P.; Zhao, H.; Chen, Y.; Jiang, L.; Ma, P. X. Methacrylate-ended Polypeptides and Polypeptoids for Antimicrobial and Antifouling Coatings. *Polym. Chem.* **2017**, *8*, 6386–6397.

(29) Mingeot-Leclercq, M.-P.; Glupczynski, Y.; Tulkens, P. M. Aminoglycosides: Activity and Resistance. *Antimicrob. Agents Chemother.* **1999**, *43*, 727–737.

(30) Yuan, H.; Yu, B.; Fan, L.-H.; Wang, M.; Zhu, Y.; Ding, X.; Xu, F. J. Multiple Types of Hydroxyl-Rich Cationic Derivatives of PGMA for Broad-Spectrum Antibacterial and Antifouling Coatings. *Polym. Chem.* **2016**, *7*, 5709–5718.

(31) Huang, Y.; Ding, X.; Qi, Y.; Yu, B.; Xu, F.-J. Reduction-Responsive Multifunctional Hyperbranched Polyaminoglycosides with Excellent Antibacterial Activity, Biocompatibility and Gene Transfection Capability. *Biomaterials* **2016**, *106*, 134–143.

(32) Wang, B.; Xu, Q.; Ye, Z.; Liu, H.; Lin, Q.; Nan, K.; Li, Y.; Wang, Y.; Qi, L.; Chen, H. Copolymer Brushes with Temperature-Triggered, Reversibly Switchable Bactericidal and Antifouling Properties for Biomaterial Surfaces. *ACS Appl. Mater. Interfaces* **2016**, *8*, 27207–27217.

(33) Liu, Y.; Ai, K.; Lu, L. Polydopamine and Its Derivative Materials: Synthesis and Promising Applications in Energy, Environmental, and Biomedical Fields. *Chem. Rev.* **2014**, *114*, 5057–5115.

(34) Yeroslavsky, G.; Girshevitz, O.; Foster-Frey, J.; Donovan, D. M.; Rahimpour, S. Antibacterial and Antibiofilm Surfaces through Polydopamine-Assisted Immobilization of Lysostaphin as an Antibacterial Enzyme. *Langmuir* **2015**, *31*, 1064–1073.

(35) Lin, J.; Chen, X.; Chen, C.; Hu, J.; Zhou, C.; Cai, X.; Wang, W.; Zheng, C.; Zhang, P.; Cheng, J.; Guo, Z.; Liu, H. Durably Antibacterial and Bacterially Antiadhesive Cotton Fabrics Coated by Cationic Fluorinated Polymers. *ACS Appl. Mater. Interfaces* **2018**, *10*, 6124–6136.

(36) Chen, R.; Willcox, M. D.; Ho, K.; Smyth, D.; Kumar, N. Antimicrobial Peptide Melimine Coating for Titanium and Its in Vivo Antibacterial Activity in Rodent Subcutaneous Infection Models. *Biomaterials* **2016**, *85*, 142–151.

(37) Wlodkowic, D.; Skommer, J.; Darzynkiewicz, Z. SYTO Probes in The Cytometry of Tumor Cell Death. *Cytometry, Part A* **2008**, *73A*, 496–507.

(38) Vitale, M.; Zamai, L.; Mazzotti, G.; Cataldi, A.; Falcieri, E. Differential Kinetics of Propidium Iodide Uptake in Apoptotic and Necrotic Thymocytes. *Histochemistry* **1993**, *100*, 223–229.

(39) Xu, Q.; Li, X.; Jin, Y.; Sun, L.; Ding, X.; Liang, L.; Wang, L.; Nan, K.; Ji, J.; Chen, H.; Wang, B. Bacterial Self-Defense Antibiotics Release from Organic-Inorganic Hybrid Multilayer Films for Long-Term Anti-Adhesion and Biofilm Inhibition Properties. *Nanoscale* **2017**, *9*, 19245–19254.